23rd ABCM International Congress of Mechanical Engineering
December 6-11, 2015, Rio de Janeiro, RJ, Brazil

COMPUTER SIMULATION OF NATURAL CONVECTION IN A SQUARE CAVITY CONTAINING A HOT BODY

Vitor José das Neves Rodrigues
Jian Su
Nuclear Engineering Program, COPPE
Universidade Federal do Rio de Janeiro(UFRJ)
21941-972, Rio de Janeiro, RJ
vrodrigues@nuclear.ufrj.br
sujian@nuclear.ufrj.br

Abstract. *Natural convection in an enclosure is relevant to many industrial and environmental applications such as heat exchangers, nuclear and chemical reactors, cooling of electronic equipment, and stratified atmospheric boundary layers. A two-dimensional study for natural convection in an enclosure with a bottom wall at constant high temperature, a top wall at constant low temperature and a hot body inside the enclosure will be simulated numerically by using a tool of computational fluid dynamics (CFD), ANSYS CFX 15.0.The objective of the work is to study the influence of the geometry of the body, position of the body in the enclosure, fluid properties and mainly the temperature difference between the walls, in terms of Prandtl and Rayleigh numbers. Steady-laminar, transient laminar and turbulent flow will be identified. Spectral analysis of instantaneous velocities and temperature by using FFT was performed for identify periodic or chaotic transient-laminar regimes.*

Keywords: *natural convection, computational fluid dynamics …*

1. INTRODUCTION

There are two elementary classes of natural convection flows in enclosures. The first is a vertical cavity with two vertical walls at different temperatures and with adiabatic horizontal surfaces.The second class of natural convection flows is a horizontal cavity with heating from below. Natural convection in a horizontal layer of fluid is the classic Rayleigh-Bénard (RB) convection and is relevant in practical problems of electronic equipment cooling, heat exchanger design, meteorology of the Earth' s atmospheric boundary layers, and so on.

Most of the previous studies on natural convection considered the classic case of thermal convection between the bottom hot and top cold walls, without any obstacles between them. There has been little study on the natural convection process with a body placed between the bottom hot and top cold walls.

It is important to consider natural convection in complicated geometries in a variety of engineering/industrial fields, such as the cooling systems of electronic devices, nuclear reactors, and steel-making processes. For example, an accurate understanding of stratified natural convection phenomena is very important in designing and optimizing the heat removal system of a fast sodium reactor. Thus, Choi and Kim [1] analyzed the turbulent natural convection in a shallow enclosure with elliptic blending second-moment closure. A driving mechanism of the energy transport in the passive auxiliary feedwater system (PAFS) of the PWR is another example of the natural convection [2]. The melting pool in the reactor vessel during severe accidents is another application.

Deardorff and Willis [3] and Lipps and Somerville [4] carried out the two-dimensional direct numerical simulation (DNS) on RB convection. The results provided detailed information on the two-dimensional fluid flow and heat transfer. However, the heat transfer rate (Nusselt number) and the critical Rayleigh number for the transition from laminar to turbulent flow, which were obtained from their two-dimensional calculations, were higher than those obtained from the experimental study given by Willis and Deardorff [5]. Ozoe et al. [6] carried out three-dimensional,laminar natural convection calculations using the fnite difference method for a fluid of Prandtl number equal to 10 at different Rayleigh numbers less than 10^4. They compared the flow and heat transfer characteristics for three diferente geometries of cubical box, infnite horizontal plates, and square channel heated from below. Lipps [7] and Grorzbach [8] carried out three-dimensional DNS of RB convection in air over a wide range of Rayleigh numbers. Their investigation covered thermal convection in three different regimes: (i) steady two-dimensional convection, (ii) time-periodic convection, and (iii) aperiodic convection. Their numerical results agreed generally well with the available experimental data and theoretical predictions. Balachandar et al. [9] and Balachandar and Sirovich [10] have computed RB convection at high Reynolds numbers in the hard turbulence regime and obtained probability distribution functions, which were then compared with corresponding experimental results. Eidson [11] conducted a numerical simulation of turbulent RB natural convection using the large eddy simulation (LES) method and compared various average properties of the resulting flow field with experimental data. The use of a LES method allowed a higher value of Rayleigh number to be simulated than was previously possible with DNS. Kenjeres and Hanjalic [12] investigated RB convection at high Rayleigh numbers up to 10^9 using the transient Reynold-averaged Navier-Stokes (TRANS) approach. This study calculated the mean flow properties, wall heat transfer, and second-moment turbulence statistics, and compared them with the available DNS and experimental data using several criteria. Kenjeres and Hanjalic [12] regarded TRANS as a very large eddy simulation (VLES) combining the rationale of the LES and of RANS modeling.

In addition, many researchers also have been interested in the characteristics of natural convection that occur due to the presence of an inner hot body placed in an enclosure. Asan [13] numerically studied 2-D natural convection in an annulus between two isothermal concentric square ducts. The results showed that the dimension ratio and Rayleigh number have a significant influence on the flow and thermal fields. Kumar De and Dalal [14] considered the problem of natural convection in an enclosure with a hot square cylinder tilted rotationally in the Rayleigh number range of 10^3 to 10^6. They considered three different height-to-width aspect ratios of the enclosure and an inner square cylinder placed at different Heights from the bottom. Their results revealed that the flow pattern and thermal stratification are modified depending on the location of the square cylinder, and the overall heat transfer changes as a function of the aspect ratio. Kim et al. [15] recently investigated the natural convection induced by a temperature difference between a cold outer square cylinder and a hot inner cylinder for different Rayleigh numbers in the range of 10^3 to 10^6 . The location of an inner circular cylinder was changed vertically along the centerline of the square enclosure. They reported that the numerical solutions for the flow and thermal fields eventually reach the steady state for all Rayleigh numbers considered. The number, size, and formation of the convection cells strongly depended on the Rayleigh number and the position of the inner circular cylinder. Ha et al. [16] studied the problem of 2-D and unsteady natural convection in a square enclosure with a square body located at the center of the enclosure. They described the characteristics of convection structures distributed in the enclosure according to the thermal boundary conditions of the inner square body imposing an adiabatic or isothermal condition. Lee et al. [17] studied the natural convection in a horizontal layer of fluid heated from below and cooled from above, which had a periodic array of evenly-spaced square cylinders occupying the layer. They reported that the transition from quasi-steady to unsteady convection depends on the presence of bodies and the aspect ratio of the cell.

In many engineering applications, the situation frequently arises wherein diverse thermal boundary conditions are imposed on walls of an enclosure. Therefore, many studies have considered the effect of a thermal boundary condition on natural convection. Corcione [18] studied natural convection in an air-filled rectangular enclosure heated from below and cooled from above with respect to variable thermal boundary conditions imposed on the side walls. The author reported that bidirection differential heating has a significant effect on the flow mode transition of natural convection in the horizontal cavity. Kandaswamy et al. [19] numerically studied unsteady laminar natural convection in an enclosure with partially heated side walls and an inner body as an internal heat source. They investigated the effects of the aspect ratio of the enclosure, different Prandtl numbers, and locations of the thermally active part of the side walls. They described the flow structure and the heat distribution in the enclosure, and the profile of the convection velocity in the mid-plane of the enclosure, for various simulation parameters. In addition, they assessed the heat transfer rate from walls of the enclosure. Aydin and Yang [20] numerically investigated the natural convection in a vertical square cavity with localized isothermal heating from below and symmetrical cooling from the side walls. They considered various length of the local heating zone as a main simulation parameter. They reported that the Nusselt number on the heated part of the bottom wall increases with increasing Rayleigh number and with the length of the heating zone. Basak et al. [21] studied the effects of thermal boundary conditions in a square enclosure on buoyancy-induced convection flow with respect to fluids with different Prandtl numbers by using the finite element method. They imposed a non-uniform heating condition on the bottom wall. They reported that the non-uniform heating of the bottom wall produces a greater heat transfer rate in the center region of the bottom wall than the rate produced in the uniform heating case for the Rayleigh. Further, a moderate range of Rayleigh numbers ($Ra = 10^3$-10^6) have been applied. In this range, the flow can reach an invariant steady state or a chaotic/periodic oscillating state as a final state according to Ra and Pr.

In the present study, we investigate the fluid flow and heat transfer characteristics of natural convection with a body at the center between two isothermal walls over a range of Rayleigh numbers. The results of natural convection with a body are compared with those of both in different vertical location, to see the effects on the fluid flow and heat transfer in the system by comparing their isotherms and streamline distribution.

2. NUMERICAL METHODOLOGY

The system consists of a horizontal layer of fluid heated from the bottom and cooled from above. The fluid layer has height L, within which a square body with sides of length W equal to L/3 and a cylinder body with radius R equal to L/5,located vertically in 0 and 0,25L with Pr 0,7 and Pr 7, both kept at a constant high temperature of T_h. The bottom wall is kept at same conditions of the body, whereas the top wall of the fluid layer is kept at a constant low temperature of T_c. The left and right side walls are assumed to be insulated. The geometry is assumed to be invariant along the z direction and thus the system represents a two-dimensional shape. The fluid properties are also assumed to be constant, except for the fluid density in the buoyancy term, which follows the Boussinesq approximation. The gravitational acceleration acts in the negative y-direction. The schematic of a two-dimensional rectangular enclosure with a body and the coordinate system is shown in Figure 1.

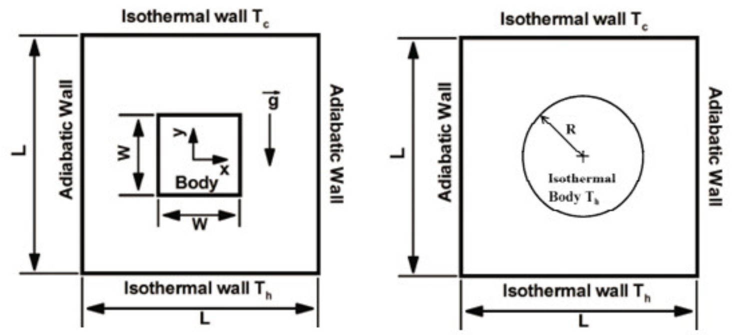

Figure 1: A schematic of the system.

We solve the continuity, Navier-Stokes and energy equations in their non-dimensional forms defined as

$$\frac{\partial u_i}{\partial x_i} = 0 \tag{1}$$

$$\frac{\partial u_i}{\partial t} + u_j \frac{\partial u_j}{\partial x_j} = -\frac{\partial p}{\partial x_i} + Pr\frac{\partial^2}{\partial x_j \partial x_j} + RaPr\theta\,\delta_{i2} \tag{2}$$

$$\frac{\partial \theta}{\partial t} + u_j \frac{\partial \theta}{\partial x_j} = \frac{\partial^2 \theta}{\partial x_j \partial x_j} \tag{3}$$

The dimensionless variables in the above equations are defined as

$$t = \frac{t^* \alpha}{L^2} \quad x_i = \frac{x_i^*}{L} \quad u_i = \frac{u_i^* L}{\alpha} \quad P = \frac{P^* L^2}{\rho \alpha^2} \quad \theta = \frac{T - T_c}{T_h - T_c} \tag{4}$$

In the above equations, ρ and α represent the density and thermal diffusivity. The superscript * in Eq. (4) represents the dimensional variables. u_i ; p, and θ are the nondimensional velocity, pressure, and temperature. The above nondimensionalization results in two dimensionless parameters: $Pr = {}^{v}/_{\alpha}$ and $Ra = {}^{g\beta L^3 (T_h - T_c)}/_{v\alpha}$ where v and β are the kinematic viscosity and volume expansion coefficient.

The local, surface-averaged, and time- and surface-averaged Nusselt number at the top and bottom walls are defined as

$$N_u = \frac{\partial \theta}{\partial n} \qquad \overline{Nu} = \int_0^1 Nu\, dS \qquad \langle \overline{Nu} \rangle = \frac{1}{t_p}\int_0^{t_p} \overline{Nu}\, dt \tag{5}$$

where n is the normal direction to walls and t_p is the period of time integration.

For the velocity field, the no-slip and no-penetration boundary conditions are imposed on the walls. The hot and cold wall temperatures of θ = 0 and 1 are imposed on the top and bottom walls, respectively. We consider four different cases of (1) square body with Pr 0,7 and located vertically in 0, (2) square body located vertically in 0,25L, (3) cylinder body with Pr 0,7 and located vertically in 0 (4) square body with Pr 7 and located in y equal to investigate the effect of the geometry of the body, vertical location and the fluid on the flow and thermal fields in the system.

The problem is all solved in software CFX 15, the creation of the geometry and the mesh. Before start the simulation of our cases, other simulations were realized to validate and compare the precision of our code, which presents good precision with the cases in the reference. Figure 2 shows the meshes created.

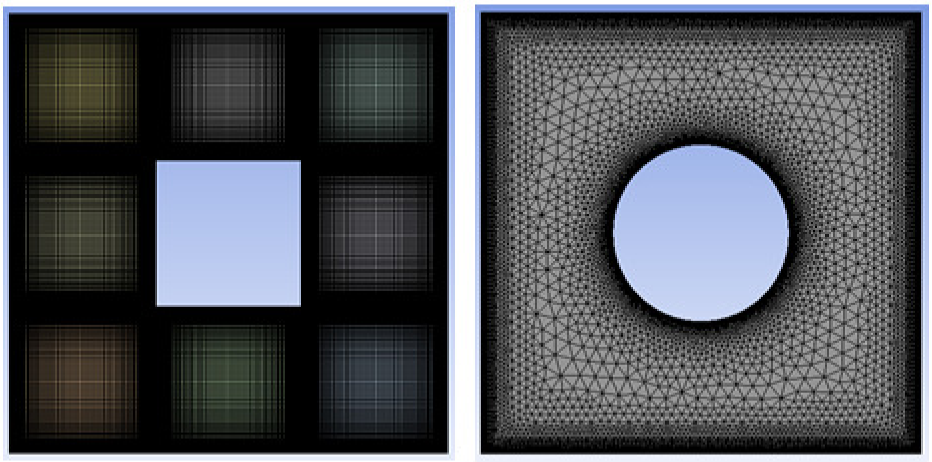

Figure 2: Mesh.

The mesh of square body is 402x402 elements and cylinder contains 285000 elements. A test of converge was realized to choice de best mesh to simulated.

3. RESULTS AND DISCUSSION

In this chapter we analyze the fluid flow and temperature fields according to the Rayleigh number.

3.1. Ra= 10^3

The fluid flow and temperature fields are steady and symmetric across the vertical centerline for the four cases study. Due to the presence of the hot body the isotherms move upward, giving rise to a stronger thermal gradient in the upper part of the enclosure and to a much lower thermal gradient in the lower part. Thus the dominant flow is in the upper half of the enclosure. The surface-averaged Nusselt numbers reach the steady state without any starting oscillatory transients.

3.2. Ra= 10^4

When the Rayleigh number increases to 10^4, only the case of square body centered with Pr 0,7 present changes and becomes no symmetric, the other cases still equal for Ra 10^3 .

The two vortices in the enclosure merge with a single vortex circulating in the clockwise direction. The fluid temperature near the right side of the hot body is higher than that near the right adiabatic wall, due to heat transfer from the hot body. Thus the flow near the right side of the body moves upward and forms the small clockwise vortex embedded in the main clockwise vortex. We can also observe the secondary counterclockwise vortex at the left top corner. The averaged-Nusselt number presents an oscillatory transient, show in the figure 3.

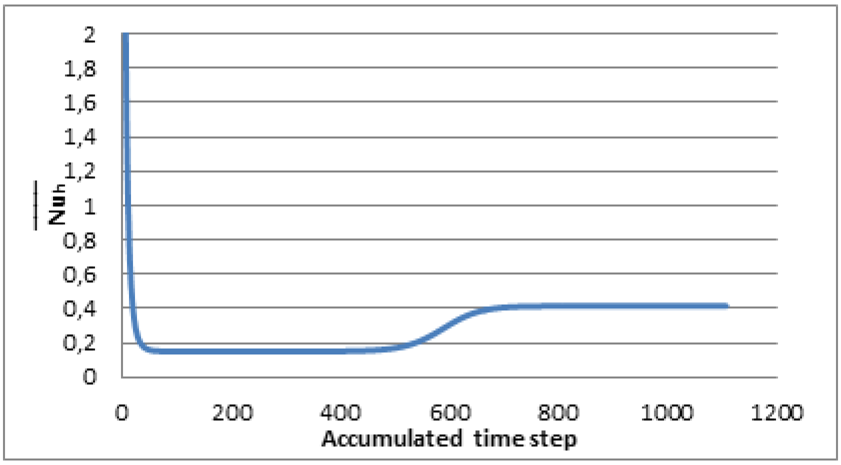

Figure 3: Averaged-Nusselt number for the centered square body at the hot wall, Pr=0,7.

3.2. Ra= 10^5

When Ra = 10^5 figure 4 ,the fluid flow and thermal fields become time dependent for square centered body with Pr 0,7, but for all other cases they reach steady state with oscillatory transient and are symmetric. Figure shows the surface-averaged Nusselt number for time dependent case.

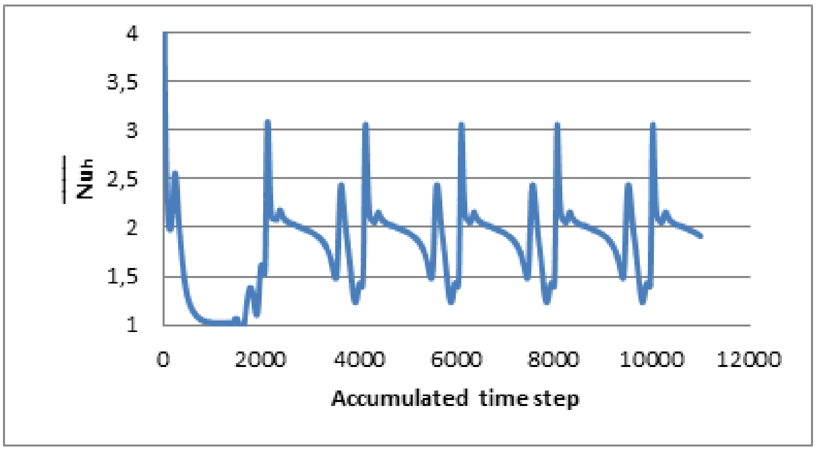

Figure 4: Averaged-Nusselt number for the centered square body at the hot wall, Pr=0,7.

For the stead state cases the temperature of the fluid is distributed throughout the cavity and surrounding the body, not getting more concentrated in the upper half only.

The time-averaged streamlines in the enclosure circulate further in the clockwise direction. The size of the clockwise vortices close to the right side of the body and of secondary vortices at the left top corner increases, due to increasing convection velocity with increasing Rayleigh number. Due to this distribution of time-averaged flow fields, the time-averaged isotherms also rotate further in the clockwise direction. The thermal gradient at the upper part in the left cannel decreases due to the effect of increasing size of counterclockwise secondary vortices. The thermal gradients at the top and bottom walls and around the hot body increase with increasing Rayleigh number, resulting in an increasing heat transfer rate.

3.4. Ra= 10^6

At Ra = 10^6, the fluid flow and temperature fields are time dependent for all situations. The gradients of time-averaged isotherms near the bottom hot and top cold walls and around the hot body increase with increasing Rayleigh number. The time-averaged isotherms change their shape again, and tend to the symmetric ones across the vertical centerline from the nonsymmetric in the square body centered with Pr 0,7. In the case of displaced square body, the shape loses the symmetry. In the figure 5 we can see surface-averaged Nusselt number.

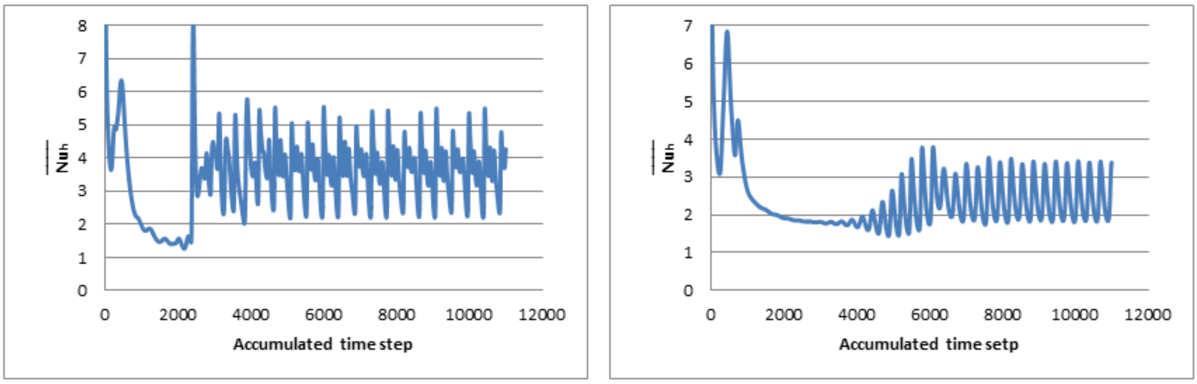

Figure 5: Averaged-Nusselt number for square body y=0 and 0,25L at the hot wall, Pr=0,7.

3.5. Ra= 10^7

The situations of square body and Pr 0,7, the isotherms and streamlines lose all the tendency of reach the symmetry. One series of vortices starts to develop in the cavity and a dominant velocity appears in the streamline. Figure 6 shows de surface-averaged Nusselt number, as you can see the graphs do not show periodic behavior.

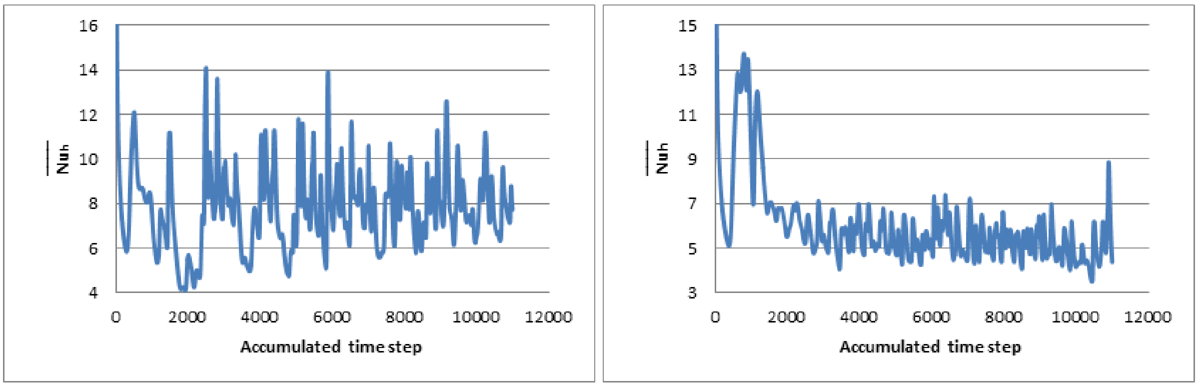

Figure 6: Averaged-Nusselt number for the centered square body at the hot wall, Pr=0,7.

3.6. Time- and Surface-Averaged Nusselt Numbers

The figures next show the time- and surface-averaged Nusselt number at bottom wall in function of Rayeligh number.

In the figure 7 are show the comparison of the vertical position for Nusselt number when the body is square and Pr 0,7. As can be seen, driving increases with the Rayleigh number for the two situations. For low Rayleigh numbers the values of Nusselt are next, but as Rayleigh increases there is greater increase convection to the case of body-centered.

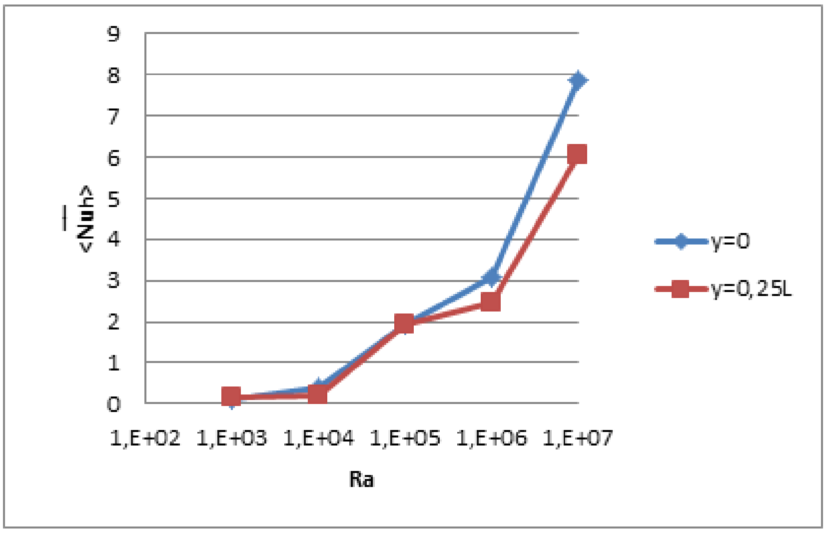

Figure 7: Time- and averaged-Nusselt number for square body as function of Rayleigh number for different vertical position at the hot wall, Pr=0,7.

Figure 8 compare the effect on the time- and surface-averaged Nusselt number for different fluids in the cavity. For down value of Rayleigh, convection is small and Nusselt values are next, with the increase of Rayleigh number, the fluid with Pr = 0.7 presents higher values but with a growth rate similar to the fluid Pr = 7.

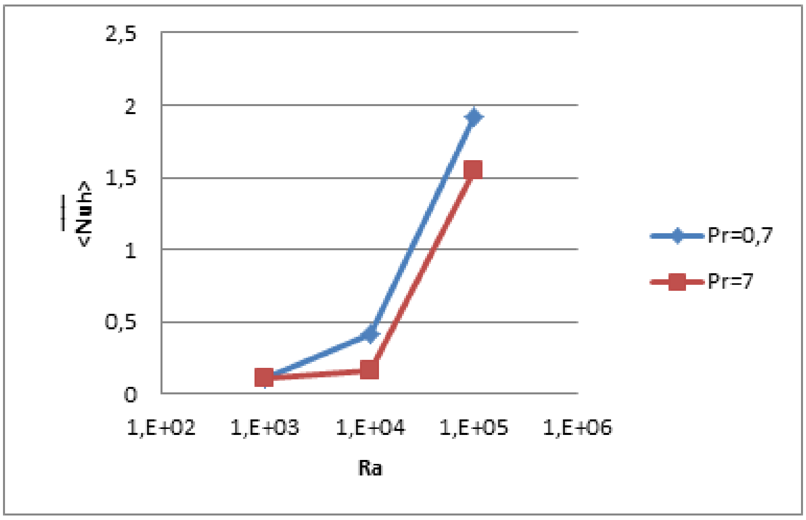

Figure 8: Averaged-Nusselt number for the centered square body as function of Rayleigh number for different fluids at the hot wall, Pr=0,7.

In the figure 9 the effect of the change in the geometry of the body, with Pr 0,7 and centered in the cavity. With the convection cylindrical body is greater than square body, as it increases the Rayleigh convection also increases for both cases, but with a much larger increment for the situation square body. For these Rayleigh numbers the solution reach the steady state, but for larger values are time dependent.

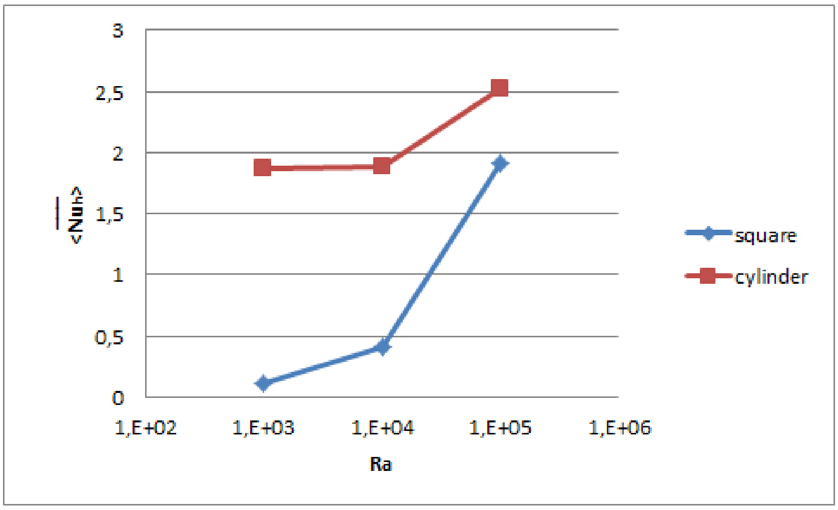

Figure 9: Averaged-Nusselt number for the centered body as function of Rayleigh number for different geometries of the body at the hot wall, Pr=0,7.

4. CONCLUSIONS

The fluid flow and temperature fields depend on geometry and position of a body and fluid in the cavity giving different streamline and isotherm patterns for varying conditions of a body. When the Rayleigh number is low, the fluid flow and temperature fields are steady, regular, and symmetric. With increasing Rayleigh number, the flow and temperature fields break their symmetry about the horizontal and vertical centerlines and the solution becomes time dependent and the time-averaged fluid flow and temperature fields become nonsymmetric. When we keep increasing the Rayleigh number to a very high value, the solution is still time dependent.

5. ACKNOWLEDGMENTS

This work was supported by the Conselho Nacional de Desenvolvimento Científico e Tecnológico(CNPq) and the Fundação de Amparo à Pesquisa do Estado do Rio de Janeiro(FAPERJ), whom I thank.

6. REFERENCES

[1]. S.K. Choi and S.O. Kim, Treatment of turbulent heat fluxes with the elliptic-blending second-moment closure for turbulent natural convection flows, International Journal of Heat and Mass Transfer, **51**, pp.2377-2388 (2008)
[2]. B.J.Yun et al. Construction Report of Separate Effect Test Facility for Passive Auxiliary Feedwater System (PASCAL), KAERI/TR-4085/2010 (2010)
[3]. J. W. Deardorff and G. E. Willis, The Effect of Two-Dimensionality on the Suppression of Thermal Turbulence, *J. Fluid Mechanics*, vol. 23, pp. 337- 353, 1965.
[4]. F. B. Lipps and C. J. Somerville, Dynamics of Variable Wavelength in Finite-Amplitude Bénard Convection, *Phys. Fluids*, vol. 14, pp. 759- 765, 1971.
[5]. G. E. Willis and J. W. Deardorff , Measurements on the Development of Thermal Turbulence in Air Between Horizontal Plates, *Phys. Fluids*, vol. 8, pp. 2225- 2229, 1965.
[6]. H. Ozoe, K. Yamamoto, S. W. Churchill, and H. Sayama, Three-Dimensional, Numerical Analysis of Laminar Natural Convection in a Confined Fluid Heated from Below, *J. Heat Transfer*, pp. 202- 207, 1976.
[7]. F. B. Lipps, Numerical Simulation of Three-Dimensional Bénard Convection in Air, *J. Fluid Mechanics*, vol. 75, pp. 113- 148, 1976.
[8]. G. Grorzbach, Direct Numerical Simulation of Laminar and Turbulent Bénard Convection,*J. Fluid Mechanics*, vol. 119, pp. 27- 53, 1982.
[9]. S. Balachandar, M. R. Maxey, and L. Sirovich, Numerical Simulation of High Rayleigh Number Convection, *J. Scientic Computation*, vol. 4, pp. 219- 236, 1988.

[10]. S. Balachandar and L. Sirovich, Probability Distribution Functions in Turbulent Convection, *Phys. Fluids*, vol. 3, pp. 919- 927, 1990.
[11]. T. M. Eidson, Numerical Simulation of the Turbulent Rayleigh- Bénard Problem Using Subgrid Modelling, *J. Fluid Mechanics*, vol. 158, pp. 245- 268, 1985.
[12]. S. Kenjeres and K. Hanjalic, Transient Analysis of Rayleigh- Bénard Convection with a RANS model, *International Journal and Heat and Fluid Flow*, vol. 20, pp. 329- 340, 1999
[13]. H. Asan, Natural convection in an annulus between two isothermal concentric square ducts, *International Communications in Heat and Mass Transfer*, 27 (2000) 367-376.
[14]. A. Kumar De and A. Dalal, A numerical study of natural convection around a square, horizontal, heated cylinder placed in an enclosure, *International Journal of Heat and Mass Transfer*, 49 (2006) 4608-4623.
[15]. B. S. Kim, D. S. Lee, M. Y. Ha and H. S. Yoon, A numerical study of natural convection in a square enclosure with a circular cylinder at different vertical locations, *Internationa Journal of Heat and Mass Transfer*, 51 (2008) 1888-1906.
[16]. M. Y. Ha, I. K. Kim, H. S. Yoon, K. S. Yoon, J. R. Lee, S. Balachandar and H. H. Chun, Two-dimensional and unsteady natural convection in a horizontal enclosure with a square body, *Numerical Heat Transfer Part A*, 41 (2002) 183-210.
[17]. J. R. Lee, M. Y. Ha, S. Balachandar, H. S. Yoon and S. S. Lee, Natural convection in a horizontal layer of fluid with a periodic array of square cylinders in the interior, *Physics of Fluids*, 16 (4) (2004) 1097-1117.
[18]. M. Corcione, Effects of the thermal boundary conditions at the sidewalls upon natural convection in rectangular enclosures heated from below and cooled from above, *International Journal of Thermal Science*, 42 (2003) 199-208.
[19]. P. Kandaswamy, N. Nithyadevi and C. O. Ng, Natural convection in enclosures with partially thermally active side walls containing internal heat sources, *Physics of Fluids*, 20 (9) (2008) 097104-1-9.
[20]. O. Aydin and W. Yang, Natural convection in enclosures with localized heating from below and symmetrical cooling from sides, *International Journal of Numerical Methods for Heat and Fluid Flow*, 10 (5) (2000) 518-529.
[21]. T. Basak, S. Roy and A. R. Balakrishnan, Effect of termal boundary condition on natural convection flows within a square cavity, *International Journal of Heat and Mass Transfer*, 49 (2006) 4525-4535.